INTERNATIONAL JOURNAL OF Telecommunications
AIR DEFENSE COLLEGE

Performance Analysis of Improved Clutter-Map MTD Processor for both Slowly & Tangential Moving Targets (STMT).

Ibrahim M. Metwally *, Tamer H.M. Soliman [1] and Hazem Z. Fahim [2]

Citation: Metwally , I.; Soliman , T.; Fahim , Z.; *Inter. Jour. of Telecommunications,* ***IJT'2022, Vol. 02, Issue 01, pp. 1-8, January 2022.*** https://ijt-adc.org/articles/2805-3044/404953

Editor-in-Chief: Yasser M. Madany.

Academic Editor: Youssef Fayad

Received: 2022-05-01.

Accepted: 2022-06-14.

Published: 2022-06-16.

Publisher's Note: The International Journal of Telecommunications, IJT, stays neutral regard-ing jurisdictional claims in published maps and institutional affiliations.

[1] AD College, Alexandria University, Egypt; thms78@gmail.com
[2] MTC, Cairo, Egypt; hkamel@mtc.edu.eg
* Correspondence: Dr.ibrahim.6914R.adc@alexu.edu.eg;

Abstract: Detection performance of slowly and tangential moving targets (STMT) is a considerable problem in modern radar systems, especially in unwanted reflected signals. These STMT produce zero/near-zero Doppler frequency shifts which the moving target indicator processor automatically removes. One popular solution is applying the received echo after passing through matched filer (MF) through a moving target detector (MTD) with a clutter map processor. In this paper, an improved clutter map MTD processor is considered. It relays on passing the output from MF through a sidelobe suppression optimum filter (SLS-OF) before clutter map MTD to relieve the detrimental effect of the clutter returns. The performance of the intended processor is evaluated compared with the traditional MTD using equal length Barker and polyphase coded waveforms. The evaluation process involves calculating the average peak signal to sidelobe ratio (PLSR) and evaluating the detection performance through the receiver operating characteristic (ROC) curve. The enhancement PLSR for the two scenarios are 4dB and 6dB, respectively, which improves the detection performance of the proposed processor by 2 dB.

Keywords: Clutter-Map; Doppler filter; Radar processor; Radar systems; Tangential targets; Zero-Velocity Filtering; Receiver Operating Characteristic

1. Introduction

The main task of radar signal processing is the detection of targets, with unknown Doppler frequency, in the existence of unwanted echoes called clutter. These targets may be fixed, moving, slowly moving, or moving tangentially to the radiated beam. Moreover, the classification of clutter may be as two classes. First, the ground clutter reflects from fixed or slowly moving objects such as trees, vegetation and artificial structure. Secondly, the environmental clutter reflects in storm clouds, precipitations, and different moving birds. It was found that while ground clutter has a very narrow spectrum, at/near-zero Doppler, the environmental clutter is more widely spread in frequency, with the center frequency being shifted noticeably away from the zero Doppler [1]. Signal processing techniques, starting from waveform design, are applied to filter out this clutter to relieve the effect of environmental conditions and thereby enhance the probability of detection (P_d) of different targets and the likelihood of false alarm (P_{fa}). Moving target detection (MTD) with clutter-map processing is an improved radar signal processor applied for this purpose. MTD achieves this improved performance due to the extensive use of Doppler filtering processes, adaptive thresholding and fine ground clutter maps [2-5].

Clutter map processing, which is a part of MTD signal processing technique, is applied to properly estimate the environmental background, and hence achieves reliable detection performance to both slowly and tangential moving targets (STMT) that are eliminated by moving target indicator (MTI) processor [6-12]. In this paper, an enhanced MTD with a clutter-map processor, by applying a derived sidelobe suppression optimum filter (SLS OP-F) cascaded with the MF, is considered. Also, we shall study the effect of using this filter on improving the detection performance of the adaptive clutter-map processing branch in an MTD processor with different

waveforms. The considered waveforms are Barker code (B_{13}) and polyphase (P_4) code, with the same length equal to 13. The block diagram of the considered radar processor is shown in Fig. (1).

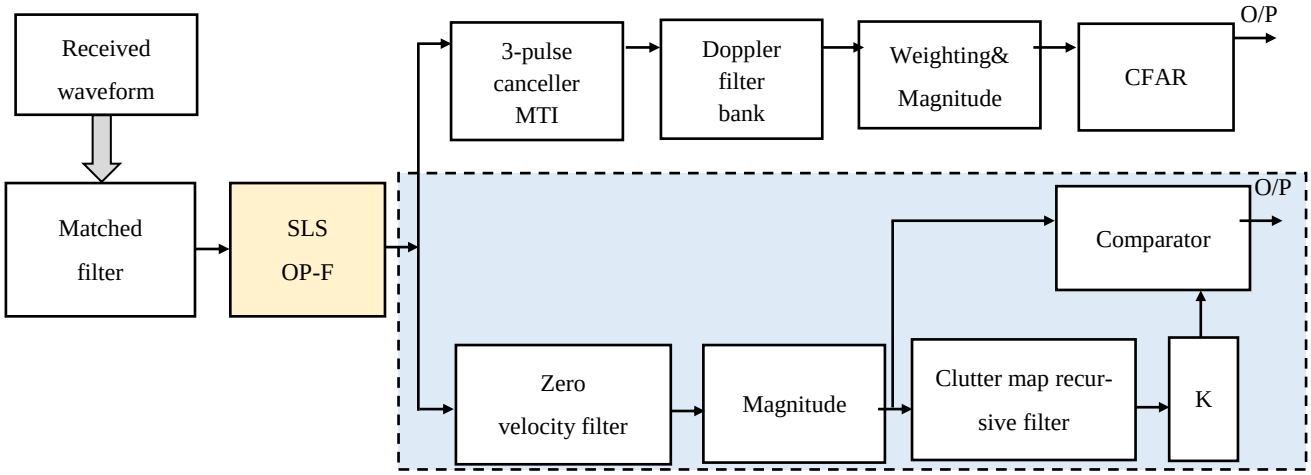

Figure 1. Proposed MDT radar processor with SLS OP-F.

The rest of the paper is listed in the following sections. First, section 2 briefly reviews the principles of radar MTD operation. Secondly, section 3 will be devoted to discussing the SLS OP-F and its universal derived formulas. Hence, the performance analysis of the proposed MTD algorithm is established in section 4. Lastly, the conclusion of the proposed work is placed in section 5.

2. Principals of radar MTD & Clutter map Operations

The area covered in modern radar systems can be demonstrated as shown in Fig. (2) [1]. The radar space is divided into various Range-Azimuth (RA) cells where both the full range and azimuth are divided into 'P' range and 'M_z' cells, respectively. As the antenna needs to spend a certain time in each of these 'M_z' azimuth rays, a fixed number of pulses always returns from each of these 'P' rang cells. The number of returned pulses, N_R, in each range azimuth cell may be calculated by [13-21].

$$N_R = \frac{F_r \theta_\beta}{\Omega}, \tag{1}$$

where F_r is the pulse repetition frequency, θ_β is the azimuth beamwidth, and Ω is the antenna scanning rate. That batch of pulses by each RA cell is called the Coherent Processing Interval (CPI), that the MTD processes. Such returned pulses must be processed rapidly to determine whether the signal returned is caused by target or clutter and noise alone. Usually, targets are discriminated from clutter by their relative Doppler shifts in the returned signal. This is achieved by implementing either pulse-Doppler processing, MTI, or MTD.

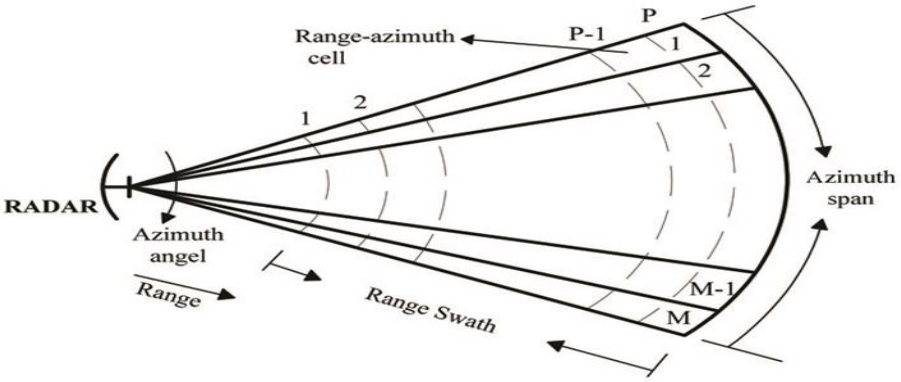

Figure 2. Radar operating environment [16].

2.1. Doppler filters bank

Doppler filter bank is the central part of the MTD signal processor. It is designed to improve target discrimination and clutter elimination. Often, it is realized by performing FFT, which relies on the DFT, for the total received data sequence, CPI. The three-pulse canceller, followed by the Doppler filter bank, as shown in Fig. 1 eliminates stationary clutter and generates N_R overlapping filters covering the total Doppler frequency interval. The detection here is based on the frequency domain. After proper thresholding, an output peak from each Doppler filter bank is detected, proclaiming the presence of the target. The location of this peak claims the corresponding Doppler frequency. The decision is always taken for every processed CPI individually.

2.2 Weighting

Generally, applying weighting to the signal in the time domain reduces the effect of leakage present at the FFT output. Different weighting functions may be used depending on the given requirements. The coefficients of the *N*-points Hamming weighting function are computed from the following equation [17]:

$$w(n) = 0.54 + 0.46\cos\left(2\pi\frac{n}{N-1}\right), n = 0, \dots, N-1 \quad (2)$$

The weighting algorithm, which is represented in the frequency domain, and corresponds to Hamming weighting function, is as follows:

$$y_m = y_m - 0.25(y_{m-1} + y_{m+1}) \quad (3)$$

Where, y_m represents the m^{th} filter output.

2.3 The Zero-Velocity Filtering (ZVF)

The function of the ZVF is the detection of targets, moving at low velocities or tangentially to the antenna pattern, whose returns exceed the level of clutter in that particular cell. The used algorithm is such that it takes the magnitude of combining the first CPI/2 inputs for both I and Q signals. Consequently, repeating this process for the second CPI/2 signal. Hence, adding the two magnitudes to form a number representing the strength of the zero-velocity component of the signal. The zero-velocity strength of a particular cell may be obtained by the following relation [1]:

$$Z = \frac{1}{2}\left\{\left|\sum_{k=1}^{CPI/2}[I(k) + jQ(k)]\right| + \left|\sum_{k=(CPI/2)+1}^{CPI}[I(k) + jQ(k)]\right|\right\} \quad (4)$$

2.4 Clutter-Map and Thresholding

The clutter map function is to create a threshold for the ZVF output. Frequently, the clutter map is constructed before the actual operation of the radar system. The reflections from fixed and moving clutters expected in the real process are measured to determine the threshold for moving targets. The average value of the ZVF output for the past scans is stored in each range cell of the ground clutter map. The map is updated recursively as follows [18]:

$$\mathrm{M}_m = (1 - \alpha)M_{m-1} + \alpha Z_m \quad (5)$$

where, M_m is the updated of the cell stored in the map, M_{m-1} is the prior value stored in that cell, and Z_m is the current output of the ZVF. Usually, the value of α is chosen to be 1/8. This means that for each scan, one-eighth of the output of ZVF is added to the seven-eighths of the previous value stored in the map. Hence, the values stored in the map are multiplied by a suitable constant, according to the required false alarm rate, to create the threshold for the ZVF output.

In MTD processing, the concept of adaptive thresholding is applied, so separate thresholds are established for each filter output. The ZVF threshold is set by the output of the clutter map multiplied by a constant [1]. As weather clutter is somewhat time-varying and extends in range over several cells, thresholding of any nonzero velocity filter is done as appropriate for an average return of that filter over several range cells. This adaptation of the threshold level leads to a form of constant false alarm rate (CFAR). Different CFAR schemes like Cell

Average (CA) CFAR, Greatest-Of (GO) CFAR, Smallest-Of (SO) CFAR, or Order Statistic (OS) CFAR may be used to obtain a background estimate that is used for thresholding [19-23]. Detection performance of clutter map and thresholding detector depends on the background statistical characteristics and the design requirements [18-25].

3. SLS OP-F and its Formulas

The SLS OP-F is a generic filter based on the concept of an inverse filter [24]. It is applicable for phase coded waveforms with any length and number of samples per subpulse. The filter coefficients are calculated using a generic formula for the filter transfer function based on the knowledge of the phase elements values of the phase coded waveforms [2,5]. In this section, the universal analytical procedure for the SLS OP-F is highlighted considering a phase coded waveform of original length (N) and phase elements with values $\emptyset = \{\emptyset_1, \emptyset_2, \dots, \emptyset_N\}$. This formula depends on the phase values of the elements that construct the phase coded waveform. Moreover, for the length of the phase sequence N is sampled with (S) samples per subpulse such that the total code length is (L=N*S); the generic formula for calculating the filter coefficients for that phase coded waveform is given by [5].

$$H_{opt}(e^{jw}) = \frac{L + \beta 1 + \gamma 1 - \gamma 2}{L + \beta 1 + \beta 2 - \beta 3} \tag{6}$$

Where,

$$\beta 1 = \sum_{i=1}^{S} [2N(i-1)]\, cos(S + 1 - i)\, \omega \tag{7}$$

$$\beta 2 = \sum_{q=1}^{N-1} \sum_{\substack{y=N \\ z=q-1}}^{\substack{N-2 \\ q+1}} \sum_{i=1}^{2S-1} \alpha_i\, cos(\emptyset_q - \emptyset_y)\, cos(\,(L - i - zS)\,\omega) \tag{8}$$

$$\beta 3 = \sum_{q=1}^{N-1} \sum_{\substack{y=N \\ z=q-1}}^{\substack{N-2 \\ q+1}} \sum_{i=1}^{2S-1} \alpha_i\, sin(\emptyset_q - \emptyset_y)\, sin(\,(L - i - zS)\;\omega) \tag{9}$$

$$\gamma 1 = \sum_{n=1}^{N-1} \sum_{m=0}^{S-1} 2m\, cos(\emptyset_n - \emptyset_{n+1}) \cos(m\omega) \tag{10}$$

$$\gamma 2 = \sum_{n=1}^{N-1} \sum_{m=0}^{S-1} 2m\, sin(\emptyset_n - \emptyset_{n+1}) sin(m\omega) \tag{11}$$

Where, α_i is a vector of coefficients with length and values of its elements depending on the S value such that the number of factors in α_i = 2S-1. Equation 6 introduces the universal formula for the SLS OP-F transfer function that calculates the OP-F coefficients that cancel the range time sidelobes of any phase-coded waveform with any length and number of samples inside each sub pulse.

4. Performance Analysis of the Enhanced MTD Processor

In this section, we are aimed to study and clarify the effect of applying the SLS OP-F, in cascade with the MF, on the detection performance of STMT [25] at the output of the MTD processor shown in Fig. 1. These STMT, which have near-zero and zero Doppler frequencies, are eliminated as a result of applying MTI processing in the upper branch of processing in the MTD processor. Therefore, it is considered a miss detected target. Thereby, the detection process of such targets is mainly achieved through the adaptive clutter-map processing branch of the MTD processor. The proposed processor is designed for a typical radar system with parameters that are listed in Table 1.

Table 1. Radar system parameters.

Radar Parameters	Parameters Value
Applied code	B13 and P4 Codes
Code length	13 Elements
Pulse repetition time	2048 μsec
Pulse repetition time	2048 μsec
Pulse width	104 μsec
Sub-pulse width	8 μsec
Intermediate frequency	30 MHz
Antenna scan rate	6rpm
Azimuth beam width	3o
Duty cycle	5%
Range resolution	1200 m

4.1 Slowly moving target detection

In this scenario, the performance of the clutter map processing branch in case of the presence of a slowly moving target is presented. The simulated target signal with (SNR=10dB) and Doppler frequency (f_d = 0.8/32f_r). The radar environment consists of Weibull distributed weather clutter with nonzero Doppler shift, which is equal to (f_{dc} = 0.3/32f_r), and covers a range volume with clutter to noise ratio (CNR = 3dB) and receiver thermal noise, which is normal Gaussian noise with zero mean and unity variance.

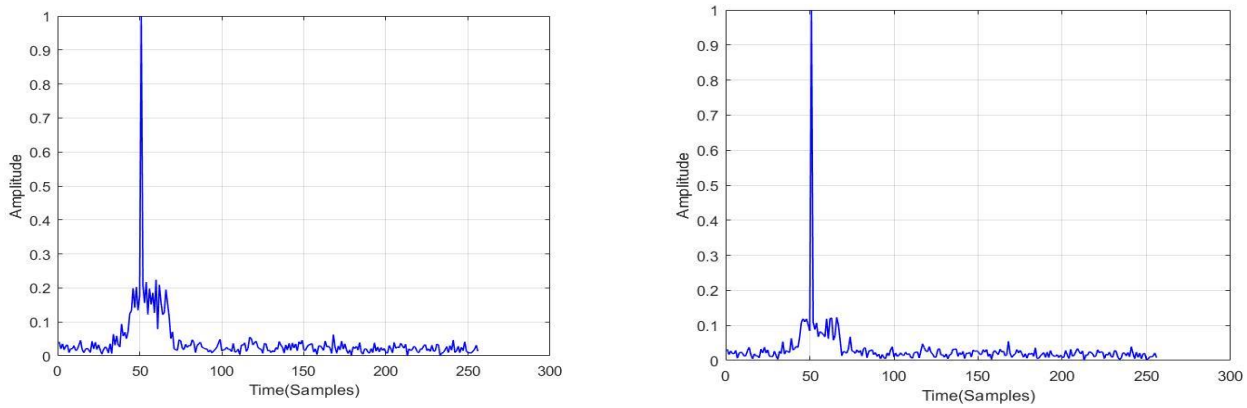

(**a**) (**b**)

Figure 3. B_{13} ZVF output for slowly moving target, they should be listed as (**a**) MF; (**b**) OP-F.

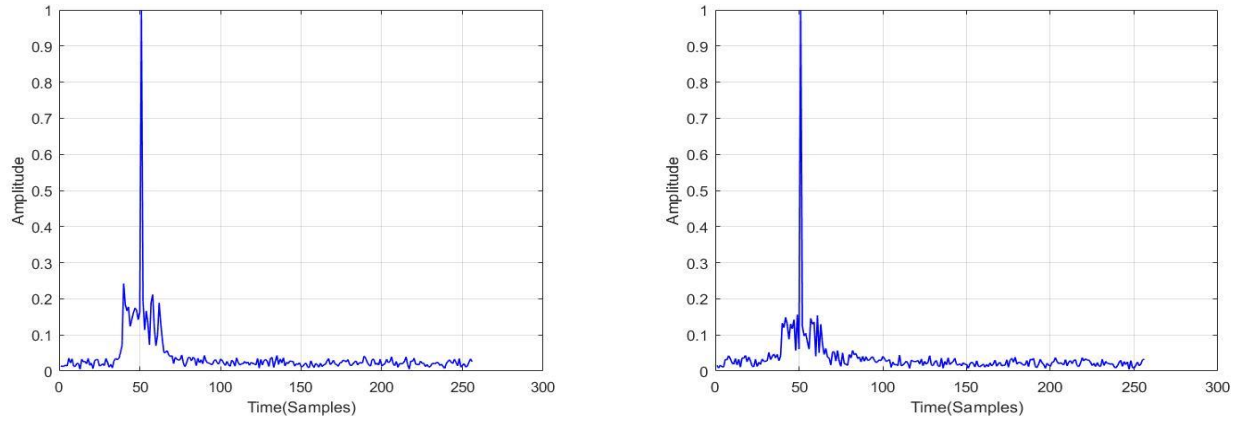

(**a**) (**b**)

Figure 4. P4 ZVF output for slowly moving target (a) MF (b) OP-F.

Table 2. ZVF average output PSLR for slowly moving target.

Radar Parameters	Average PSLR at ZVF output (dB)	
	MF	OP-F
B_{13}	12.98dB	17.07dB
P4	12.62dB	15.28dB

The simulated received signal has total signal-to-noise-plus-clutter ratio (SNCR = 6dB). The ZVF outputs of MF alone and applying SLS OP-F are shown in Fig. 3 and Fig. 4, considering both B_{13} and P4 waveforms, respectively. The average peak signal-to-sidelobe ratios (PSLR)s at the ZVF output over 1000 trials are listed in Table 2. From Fig. 3 and Fig. 4, a noticeable enhancement in the processed signal after applying the SLS OP-F relative to only MF is achieved. These signals are then fed to the clutter map adaptive filter to estimate the background and determine the proper adaptive threshold for target detection according to the required probability of false alarm (P_{fa}). Finally, the enhancement in detection performance is evaluated through the receiver operating characteristics (ROC) curve, as shown in Fig. 5 for the considered waveforms. ROC curves are plots of the probability of detection / the probability of false alarm for a given signal-to-noise ratio. Generally, these ROC curves are often used to assess the performance of a radar or sonar detector.

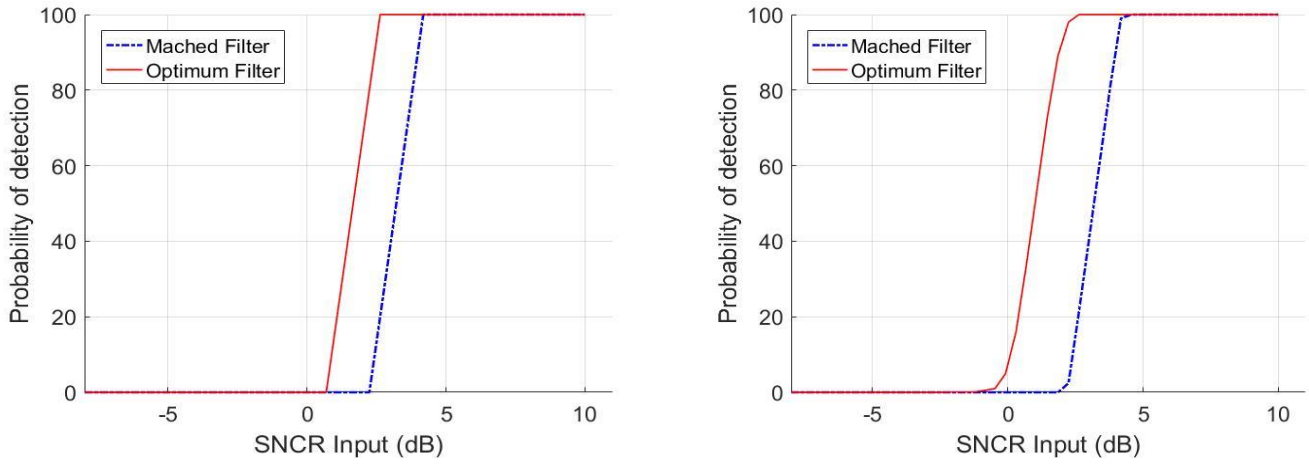

(**a**) (**b**)

Figure 5. Slowly moving target ROC curve at Pfa=10-6 (a) B13 (b) P4.

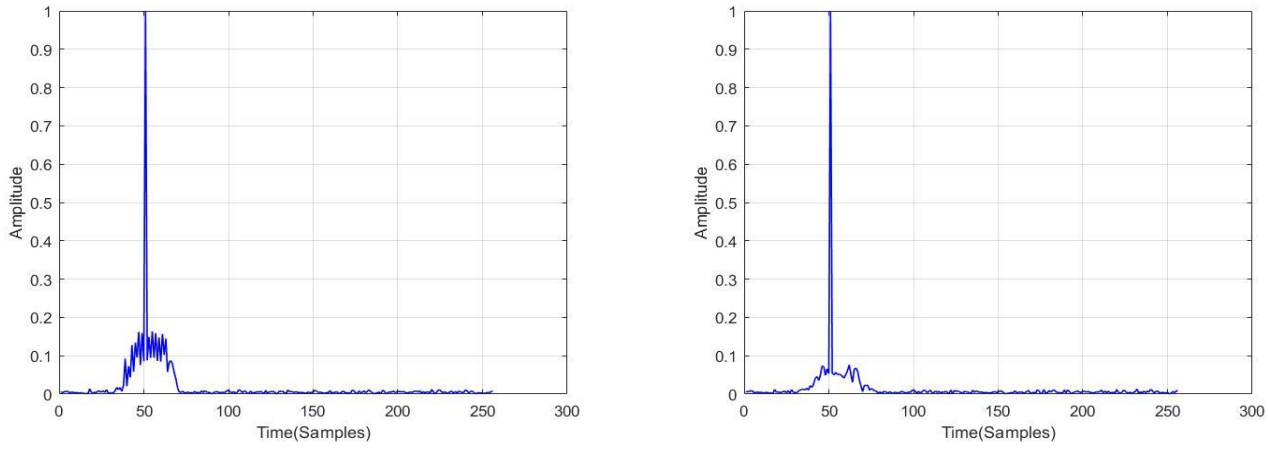

(**a**) (**b**)

Figure 6. B_{13} ZVF output for tangential target, they should be listed as (**a**) MF; (**b**) OP-F.

4.2 Tangential target detection

In this scenario, a simulated signal of the tangential target, which appears to have a zero radial velocity (i.e f_d=0) is generated. Such echo signals, which are entirely eliminated by the MTI processing module and cannot be detected in the upper branch of the MTD processor, are mainly detected by the ZVF and clutter map processor. The generated signal has SNR=5dB, f_d = 0, and is contaminated in the same Weibull weather clutter signal with CNR = 10dB.

Table 3. ZVF average output PSLR for the tangential target.

Waveform	Average PSLR at ZVF output (dB)	
	MF	OP-F
B_{13}	15.29dB	21.59dB
P4	12.80dB	18.28dB

Clutter Doppler is f_{dc} = 0.1/32f_r and receiver thermal noise such that the total SNCR of the received signal is equal to -1dB. This modification in the simulated parameters increases the effect of the clutter signal on the target signal. The outputs of ZVF for MF and OP-F consider both generated signals B_{13} and P4 displayed in Fig. 6 and Fig. 7, respectively. The average PSLRs at the ZVF output over 1000 trials are listed in Table 3. The ROC curve for this scenario is shown in Fig. 8 to clarify the detection performance enhancement for B_{13} and P4 waveforms.

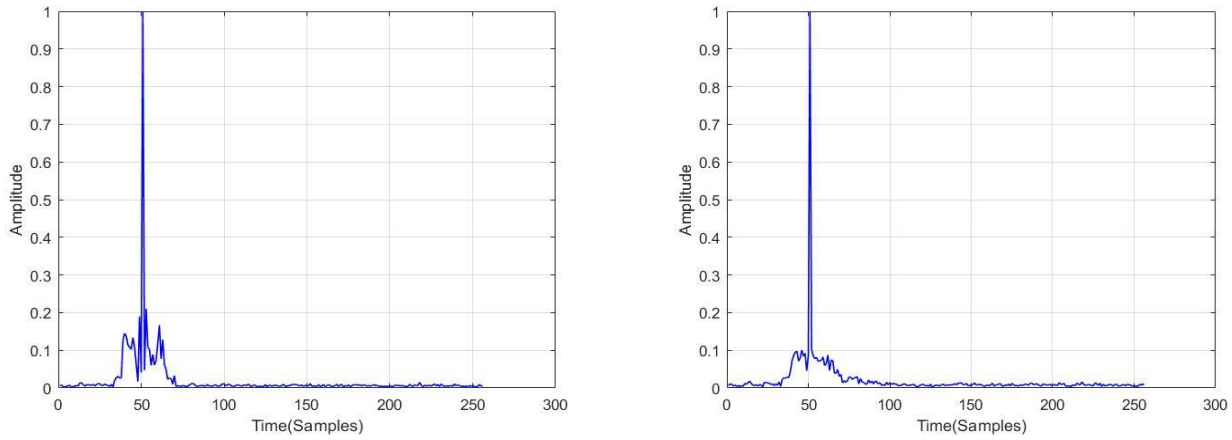

(**a**) (**b**)

Figure 7. P4 ZVF output for tangential target: (**a**) MF; (**b**) OP-F.

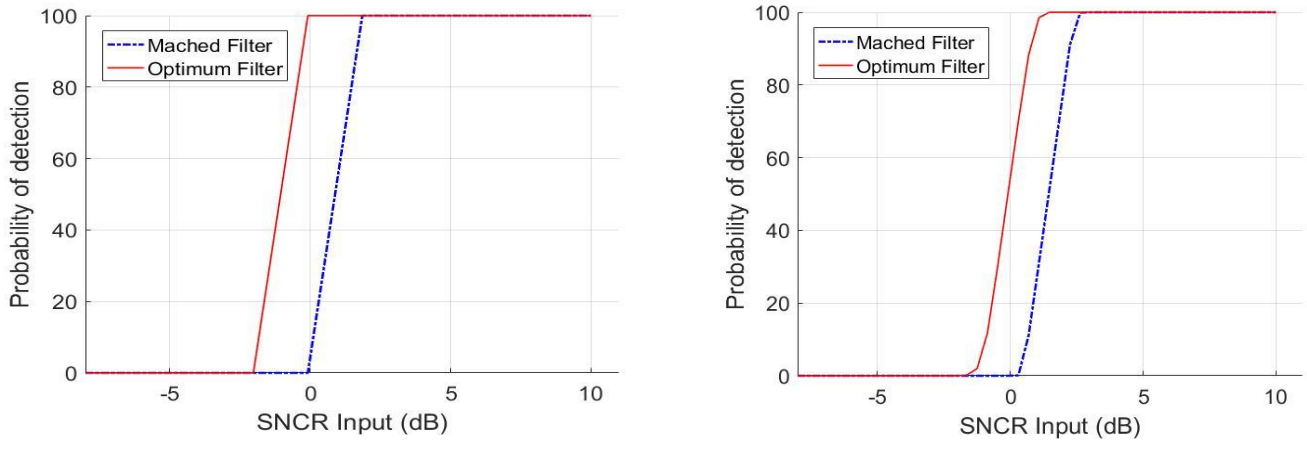

(**a**) (**b**)

Figure 8. Tangential target ROC curve at Pfa=10-6 (a) B13 (b) P4.

5. Conclusions

In this work, the effect of applying the SLS OP-F on the detection performance of the clutter map processing branch in the MTD processor with different waveforms has been achieved. Two different scenarios for echo signals are simulated as STMT is immersed in weather clutter and thermal noise. As a result, approximately 4dB & 6dB enhancement in PSLR at the output of ZVF due to applying the OP-F in case of STMT have been achieved, respectively. This enhancement in PSLR improves the detection performance of the clutter map processing branch by about 2dB while preserving $P_{fa}=10^{-6}$.

References

1. Z. Zhang, B. Chen and M. Yang. Moving Target Detection Based on Time Reversal in a Multipath Environment. *IEEE Transactions on Aerospace and Electronic Systems* **2021** vol. 57, pp. 3221 - 3236.
2. Ibrahim. M. Metwally, Abd El Rahman H Elbardawiny, Fathy M Ahmed and Hazem Z Fahim. A generic analytical formula for range sidelobes cancellation filters in pulse compression phase coded waveforms. *18th International Conference on AEROSPACE SCIENCES & AVIATION TECHNOLOGY* **2019**, pp. 9-11.
3. C. Muehe. Moving target detector, an improved signal processor. *AGARD New Devices, Tech. And Systems in Radar* **1977**.
4. C. Muehe. Advances in radar signal processing. *IEEE Electro'76, Boston* **1976**.
5. Ibrahim. M. Metwally, Abd El Rahman H Elbardawiny, Fathy M Ahmed and Hazem Z Fahim. A Universal Formula for Side-Lobes Removal Optimum Filter in Multi samples Phase Coded Pulse Compression Radars. *5th International Conference on Intelligence Systems and Informatics, (AISI2019)* **2019,** pp**.** 26-28.
6. X. Meng. Performance analysis of Nitzberg's clutter map for Weibull distribution. *Digital Signal Processing* **2010** vol. 20, pp. 916-922.
7. M. Hamadouche, M. Barakat, and M. Khodj. Analysis of the clutter map CFAR in Weibull clutter. *Signal processing* 2000 vol. 80, pp. 117-123.
8. M. Lops. Hybrid clutter-map/L-CFAR procedure for clutter rejection in nonhomogeneous environment. *IEE Proceedings-Radar, Sonar and Navigation* **1996** vol. 143, pp. 239-245.
9. M. Lops and M. Orsini. Scan-by-scan averaging CFAR. *IEE Proceedings F (Radar and Signal Processing)* **1989** pp. 249-254.
10. Xu, Shuwen, Zhexiang Wang, Penglang Shui, and Shengjie Huang. Improved clutter-map detection for radar targets in K-distributed clutter. IET International radar conference **2021** 1023-1027.
11. Van Cao, Tri-Tan. Dual estimators for clutter-map CFAR detection on non-Gaussian background. *18th IEEE International Radar Symposium (IRS)* **2017** pp. 1-10.
12. Zhou, Yi, Xiaoming Liu, Jidong Suo, Chang Liu, Xiaohong Su, and Limei Liu. Nonparametric background model based clutter map for x-band marine radar. *IEEE International Conference on Image Processing (ICIP)* **2015** pp. 123-127.
13. N. Ustalli, D. Pastina and P. Lombardo. Target Motion Parameters Estimation in forwarding Scatter Radar. *IEEE Transactions on Aerospace and Electronic Systems* **2020** vol. 56, pp. 226-248.
14. B. Edde. Radar principles, technology, applications. *NASA STI/Recon Technical Report A* **1993** vol. 93.
15. J. DiFranco and B. Rubin. Radar detection: The Institution of Engineering and Technology **2004**.
16. J. Giridhar and K. Prabhu. Implementation of MTD-WVD on a TMS320C30 DSP processor. Microprocessors and Microsystems **1998** vol. 22, pp. 1-12.
17. V. Oppenheim. Discrete-time signal processing: *Pearson Education India*, **1999**.
18. Nitzberg, "Clutter map CFAR analysis. *IEEE Transactions on Aerospace and Electronic systems* **1986** pp. 419-421.
19. S. Liu, Y. Cao, TS. Yeo, W. Wu and Y. Liu. Adaptive Clutter Suppression in Randomized Stepped-Frequency Radar. *IEEE Transactions on Aerospace and Electronic Systems* **2021** vol. 57.
20. M. Zhan, P. Huang, S. Zhu and S. Li. A Modified Keystone Transform Matched Filtering Method for Space-Moving Target Detection. *IEEE Transactions on Geoscience and Remote Sensing* **2022** vol. 60.
21. A. Moustafa, F. M. Ahmed, K. Moustafa and Y. Halwagy. A new CFAR processor based on guard cells information. *IEEE Radar Conference (RADAR)* **2012** pp. 0133–0137.
22. Ibrahim. M. Metwally, Abd El Rahman H Elbardawiny, Fathy M Ahmed and Hazem Z Fahim. Real-Time Design and Implementation of a Proposed Phase Coded radar Matched Filtering with Generic Sidelobes Suppression Optimum Filter. *12th International Conference on Electrical Engineer (ICEEG)* **2021**.
23. J. Zhong, K. Zhang, Q. Zeng and X. Liu. A False Alarm Elimination Algorithm of Foreign Objects Debris Detection Based on Duffing Oscillator. *IEEE Access* **2022** Vol. 10, pp. 7588 – 7597.
24. Daniels, R. C., and Gregers-Hansen, V. Code inverse filtering for complete sidelobe removal in binary phase coded pulse compression systems. Proceedings of IEEE International Radar Conference, May 9—12, **2005**, 256—261.
25. F. M. Ahmed. Tangential Targets Detection in LFMCW Radars. 12th International Conference on Electrical Engineering **2020.**